

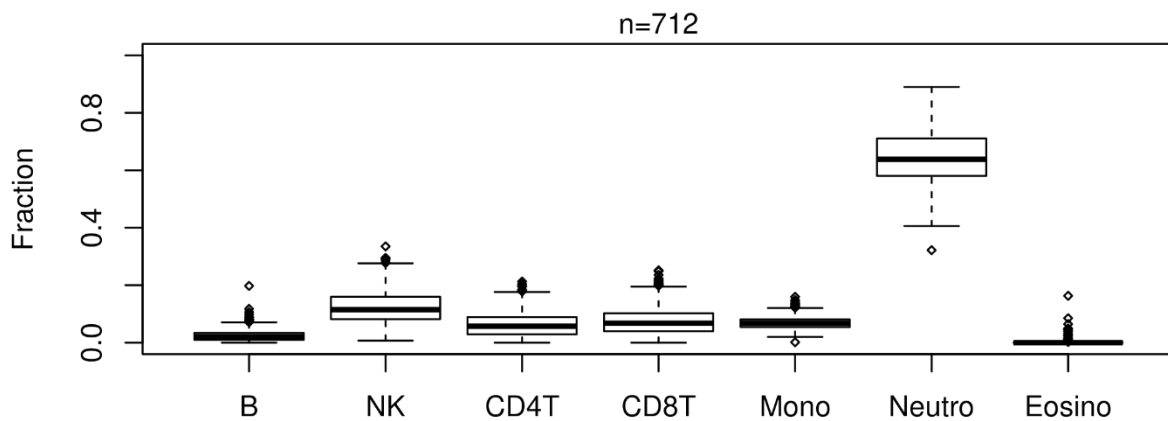
1 **Supplementary Information for “A cell-type**  
2 **deconvolution meta-analysis of whole blood EWAS**  
3 **reveals lineage-specific smoking-associated DNA**  
4 **methylation changes”**

5 You et al

6

7 **SUPPLEMENTARY FIGURES**

8



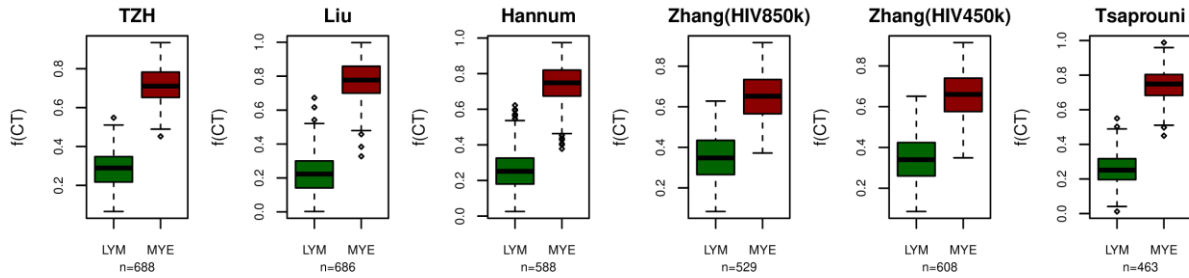
9

10 **Supplementary Figure 1: Blood cell type fraction estimates derived from EpiDISH.** Blood cell  
11 subtype fractions as estimated using the EpiDISH algorithm in the TZH cohort. Number of samples is  
12 indicated above plot. Horizontal line within boxes indicate median, box-boundaries the inter-quartile  
13 range, and whiskers extend to 1.5 times this range.

14

15

16



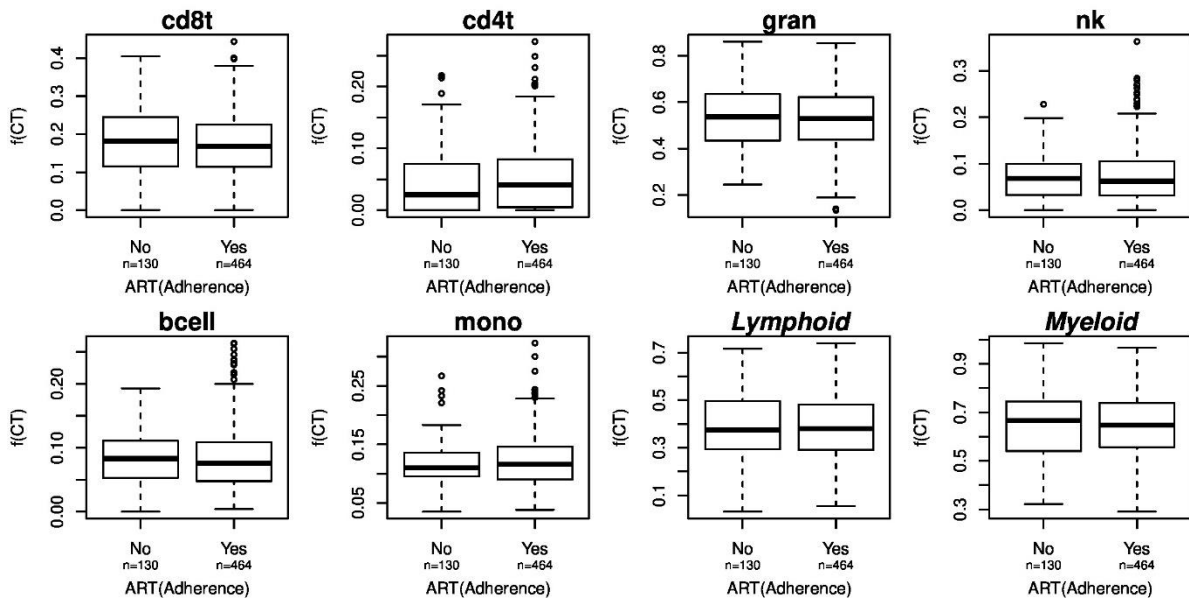
17

18 **Supplementary Figure 2: Lymphoid and myeloid fractions across all 6 whole blood cohorts.** For  
 19 each of the 6 whole blood cohorts, we used EpiDISH to estimate cell-type fractions for each of the 7  
 20 main blood cell subtypes (CD4T, CD8T, NK, B, Mono, Neu, Eosin.), which we then summarize at the  
 21 level of lymphoid and myeloid cells, as shown. Number of whole blood samples in each cohort is given.  
 22 Horizontal line within boxes indicate median, box-boundaries the inter-quartile range, and whiskers  
 23 extend to 1.5 times this range.

24

25

26

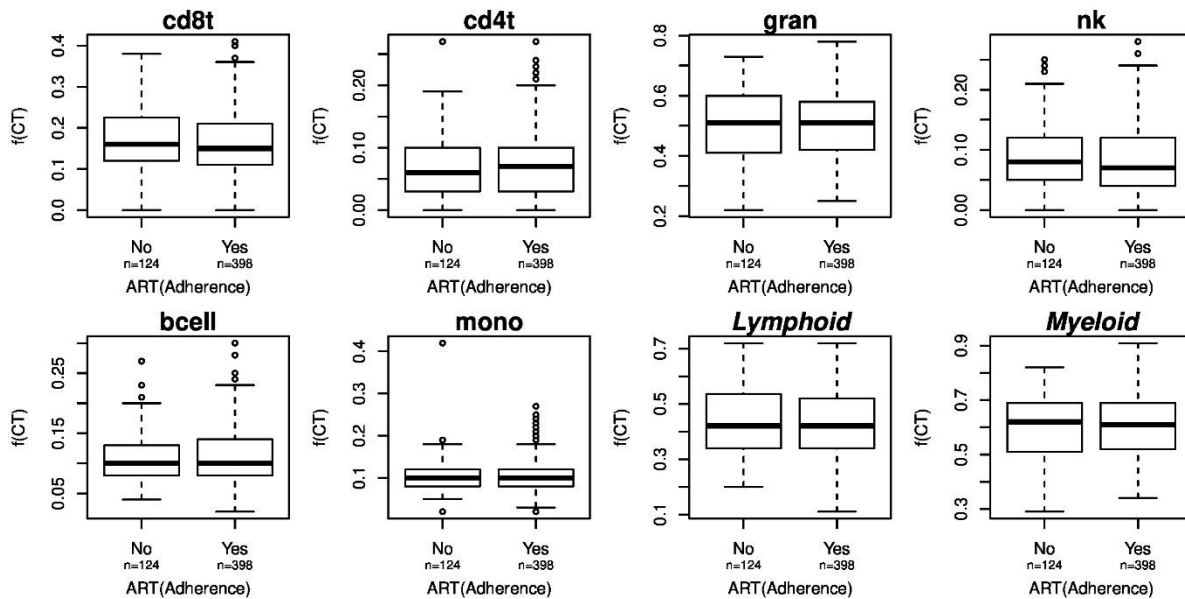


27

28 **Supplementary Figure 3: Cell-type fractions vs ART in Zhang(HIV450k).** For 6 main blood cell  
 29 subtypes and the total lymphoid and myeloid fractions, we compare corresponding cell-type fractions  
 30 (f(CT),y-axis) in the Zhang(HIV450k) cohort against adherence to anti-retroviral therapy (ART).  
 31 Number of HIV patients complying with ART or not is given. In this figure, the granulocyte fraction is  
 32 the total of neutrophil and eosinophil fraction. Horizontal line within boxes indicate median, box-  
 33 boundaries the inter-quartile range, and whiskers extend to 1.5 times this range.

34

35



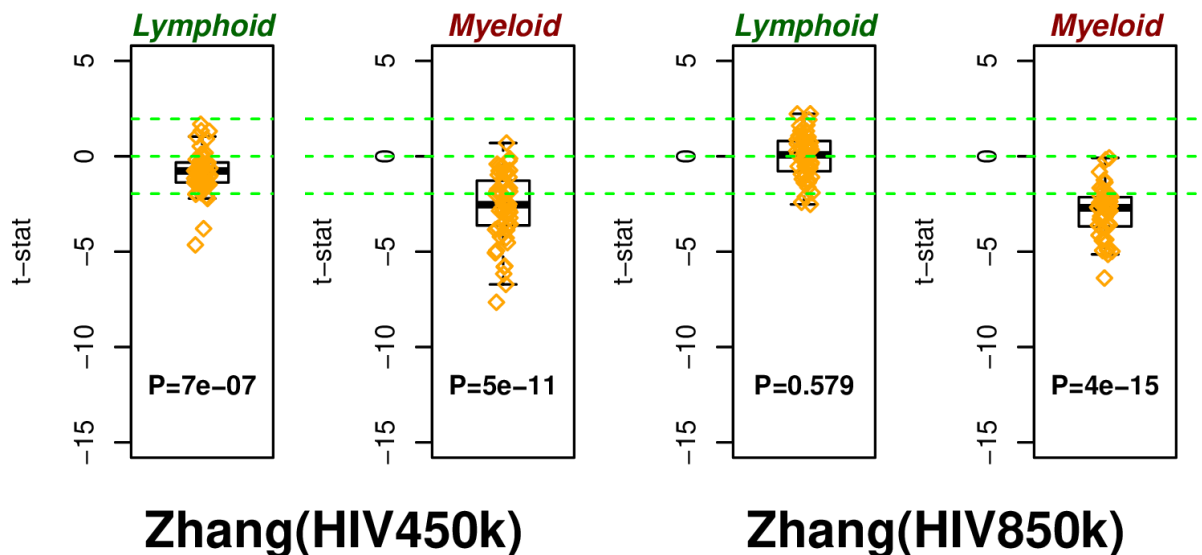
36

37 **Supplementary Figure 4: Cell-type fractions vs ART in Zhang(HIV850k).** For 6 main blood cell  
 38 subtypes and the total lymphoid and myeloid fractions, we compare corresponding cell-type fractions  
 39 ( $f(CT)$ , y-axis) in the Zhang(HIV850k) cohort against adherence to anti-retroviral therapy (ART).  
 40 Number of HIV patients complying with ART or not is given. Horizontal line within boxes indicate  
 41 median, box-boundaries the inter-quartile range, and whiskers extend to 1.5 times this range.

42

43

44



45

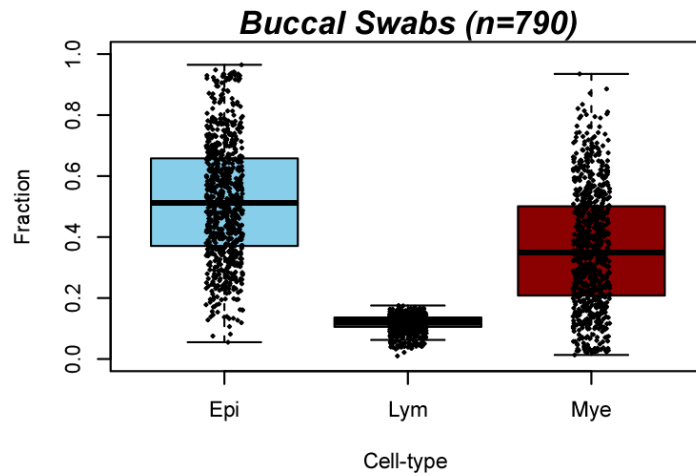
46 **Supplementary Figure 5: Cell-type specific associations of gold-standard CpGs with smoking in**  
 47 **HIV cohorts.** Boxplots of t-statistics of association of DNAm with smoking in the whole blood HIV  
 48 cohorts of Zhang et al, as derived with CellDMC for both lymphoid and myeloid lineages. Boxplots  
 49 only display the 60 gold-standard smoking hypomethylated CpGs from Gao & Brenner. P-value derives

50 from a one-tailed Wilcoxon rank sum test. Horizontal line within boxes indicate median, box-  
51 boundaries the inter-quartile range, and whiskers extend to 1.5 times this range.

52

53

54



55

56 **Supplementary Figure 6: Estimates of cell-type fractions in buccal swabs using HEpiDISH.**

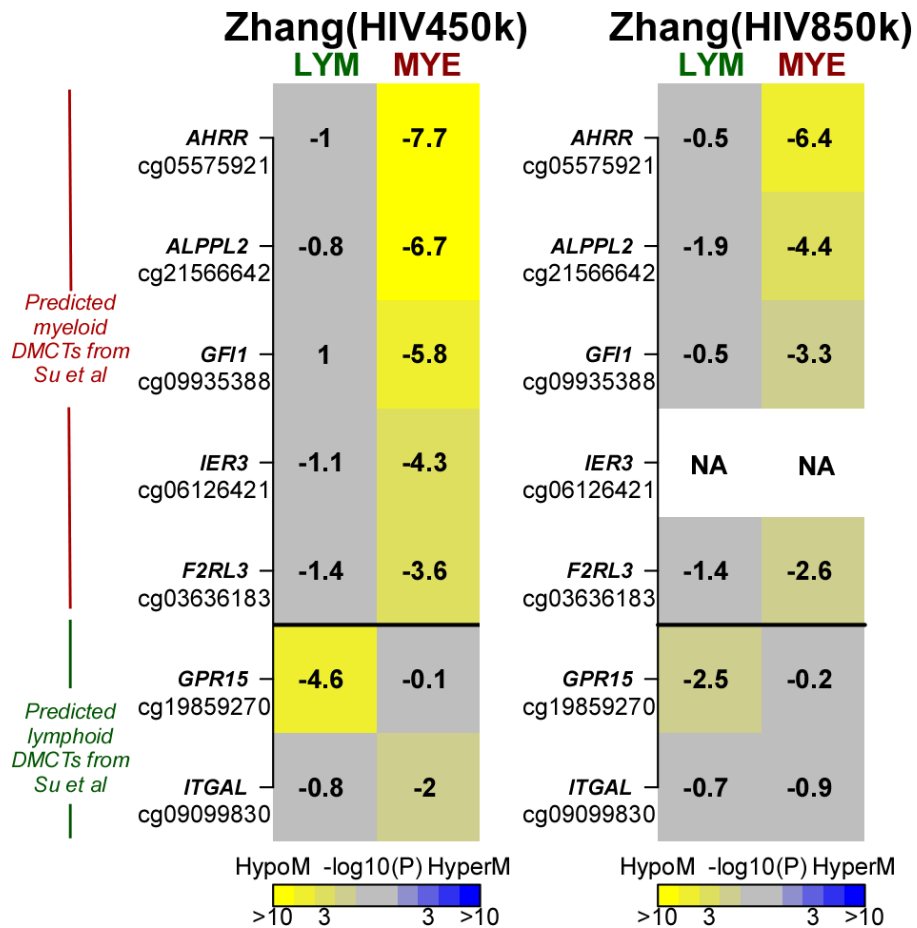
57 Estimates of the fractions of total epithelial, total lymphoid and total myeloid cells in the 790 buccal  
58 swabs. Horizontal line within boxes indicate median, box-boundaries the inter-quartile range, and  
59 whiskers extend to 1.5 times this range.

60

61

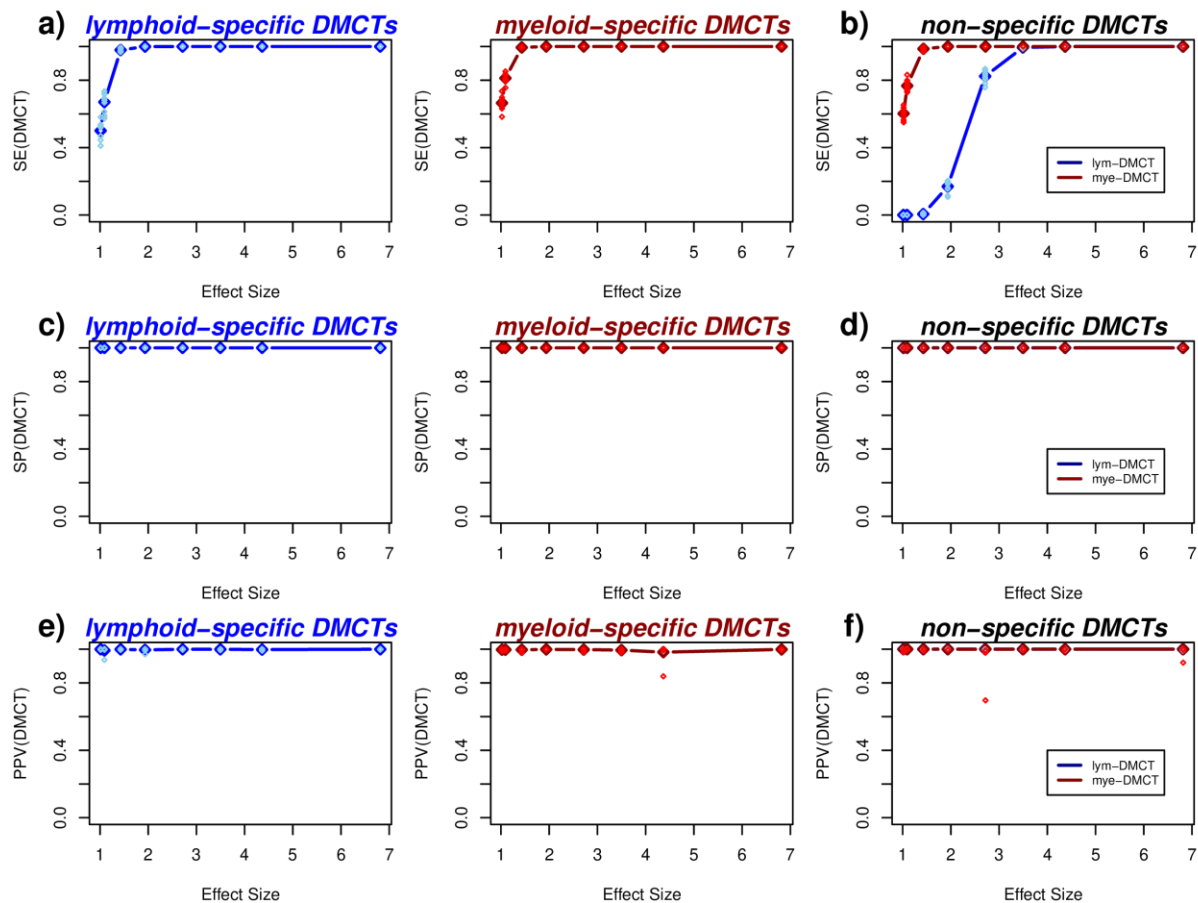
62

63



64

65 **Supplementary Figure 7: CellDMC predictions in HIV cohorts.** Heatmaps of myeloid and lymphoid  
 66 significance P-values, as derived from CellDMC, in 2 separate HIV cohorts from Zhang et al, and for a  
 67 panel of 7 CpGs which Su et al showed to exhibit myeloid and lymphoid specific hypomethylation in  
 68 smokers. Significance of P-values is denoted by color, and the corresponding t-test statistic values are  
 69 displayed in the heatmap. P-values derive from the t-test in the CellDMC model and are two-tailed.



70

71 **Supplementary Figure 8: Power estimates for simulation model using n=600. a)** Plot of the  
 72 sensitivity to detect lymphoid and myeloid specific DMCTs (y-axis) vs. the smoking effect size (x-axis).  
 73 Data points represent the mean sensitivity, as obtained over 10 different Monte-Carlo simulations,  
 74 encompassing 482077 CpGs of which 1000 are DMCTs. Datapoints are for n=600 (300 cases and  
 75 controls). Each sample is an in-silico mixture of real DNAm profiles representing one purified CD4+  
 76 T-cell and one monocyte sample. For each case sample, 1000 DMCTs at the given average effect size  
 77 in only one of the two cell-types was generated. The sensitivities for each of the 10 Monte-Carlo runs  
 78 are shown in skyblue/red. **b)** As a), but now for the scenario where the DMCTs are introduced at the  
 79 same CpG in both cell-types. Sensitivity to detect the DMCT in the lymphoid and myeloid lineage is  
 80 shown. **c-d)** As a-b), but now for the specificity. **e-f)** As a-b), but now for the precision or positive  
 81 predictive value (PPV).